COBEM 2023 27TH INTERNATIONAL CONGRESS OF MECHANICAL ENGENEERING

ABCM Brazilian Society of Mechanical Sciences and Engineering
27th ABCM International Congress of Mechanical Engineering
December 04-08, 2023, Florianópolis-SC, Brazil

COB-2023-1964
ON THE COMPATIBILITY BETWEEN EXPERIMENT AND NUMERICAL MODEL OF A THERMOACOUSTIC HEAT EXCHANGER

Geovane Costa Clemente[1]
Flávio de Campos Bannwart[2]
School of Mechanical Engineering - University of Campinas/UNICAMP
e-mails [1]g256318@dac.unicamp.br; [2]fcbannwart@fem.unicamp.br

Abstract. *Thermoacoustics studies the coupling phenomenon between heat fluxes and the oscillatory motion of resonant acoustic particles. Thermoacoustic engines achieve the spontaneous conversion of thermal energy into mechanical energy in the form of acoustics, which can then be converted into electrical energy. One advantage is their ability to regenerate low-availability thermal energy compared to conventional engines. Recent research aims to enhance this regeneration potential, focusing primarily on the heat rejection efficiency of the acoustic fluid in the engine. The objective of this work is to design a heat exchanger that maximizes the transfer of heat from the air in an acoustic regime to a refrigerant fluid affected by magnetic field interference, aiming for thermal coupling between their oscillations. For this purpose, a laminar 3D numerical model representing the heat exchanger of a stationary wave thermoacoustic engine was developed using ANSYS Fluent 2022R2 and will be validated through a corresponding experiment using water as the refrigerant fluid at room temperature, seeking compatibility between both approaches. Both experimental and numerical results indicated a model consistent with the physical phenomenon for air in free flow, and a satisfactory computational model when analyzing the oscillatory motion of acoustic particles in the air. Moreover, a greater thermal exchange effectiveness was detected for a tube with an elliptical section compared to a tube with a circular section of the same internal area.*

Keywords: *thermoacoustics, thermoacoustic engine, heat transfer, CFD, thermomagnetism, standing wave*

1. INTRODUCTION

The search for sustainable and efficient technologies has become increasingly important due to the energy crisis and environmental issues. In this context, thermoacoustics emerges as a promising alternative, representing a phenomenon that involves the coupling between heat fluxes and the oscillatory movement of resonant acoustic particles, whether in a standing or progressive wave regime (Alamir, 2021) (Chen *et al.*, 2018) (Sun *et al.*, 2013).

Operating under the plane wave acoustic condition, thermoacoustic engines are an example of a thermal engine based on the thermoacoustic phenomenon and stand out for their easy-to-build design. These engines perform the spontaneous conversion of thermal energy into mechanical energy in acoustic form, which can subsequently be converted into electrical energy. With their simple structure, high reliability, low manufacturing and maintenance costs, these engines are highly attractive for conducting new research (Allafi and Saat, 2022) (Wang *et al.*, 2015).

Thermoacoustic engines consist of several components, such as a porous solid medium known as a stack, hot and cold temperature heat exchangers located at the ends of the stack, an acoustic driver, and a resonator. Additionally, thermoacoustic engines stand out as advantageous options due to the absence of moving mechanical components and the use of eco-friendly gases. They offer a promising and sustainable pathway to energy generation, minimizing the negative impact on the environment (Saat *et al.*, 2019) (Sun *et al.*, 2013).

Heat transfer in thermoacoustic systems is mainly governed by conduction and convection, influenced by operating conditions, heat exchanger design, material properties, and working fluid characteristics. Conduction, based on Fourier's law, maintains the temperature gradient across the stack for efficient energy conversion. Convection facilitates heat exchange between the working fluid and the heat exchangers' solid surfaces, propelled by oscillatory flow, and is affected by factors like Reynolds number, Prandtl number, and the heat exchanger design.

The efficiency of a thermoacoustic device depends heavily on the effectiveness of the heat exchangers. In smaller engines with lower heat transfer, heat exchange mainly relies on thermal conduction. Therefore, thin and parallel fins made of conductive materials are used to connect the stack to the resonator. On the other hand, engines with higher thermal loads employ heat exchangers with tubes arranged in a parallel fin matrix, which enhances the contact area between the fluid and the surface, thereby optimizing heat transfer (Piccolo and Pistone, 2006).

The integration of advanced materials and innovative designs in thermoacoustic engines enhances their performance and energy efficiency. Compact and efficient engines can be developed for various energy conversion systems by exploring alternative fluids with favorable thermoacoustic properties. Moreover, the potential for integrating thermoacoustic engines with solar thermal collectors and utilizing waste heat from industrial processes further contributes to their sustainability

and reduces reliance on non-renewable energy sources (Mumith *et al.*, 2014) (Jaworski and Mao, 2013).

Studies conducted by Allafi *et al.* (2021), Saat *et al.* (2019), Piccolo *et al.* (2019), Ilori *et al.* (2018), Saat and Jaworski (2017a), Saat and Jaworski (2017b), Jaworski and Piccolo (2012), and Piccolo and Pistone (2006) have explored both experimental and numerical aspects of these systems, contributing to a comprehensive understanding of the thermodynamic and acoustic phenomena involved. These in-depth investigations have resulted in significant advancements in the search for more efficient and sustainable energy solutions.

The objective of this work is to develop a three-dimensional computational model using the CFD technique, in conjunction with the development of simple experiments, in order to conceive and analyze a heat exchanger for a thermoacoustic engine. The main goal of this analysis is to achieve compatibility between the computational and experimental approaches, aiming to understand the heat transfer phenomenon from the air in the acoustic regime to the refrigerant fluid. This involves validating the developed computational model and establishing thermal coupling between the flow of the refrigerant fluid and the oscillations of the acoustic fluid. The validation of the computational model depends primarily on the convergence between the temperature values obtained in the experimental and numerical results. The consequence of a successful compatibility is to allow the use of the computational model in future studies, covering different structural configurations and more complex flow conditions.

2. LITERATURE REVIEW

In thermoacoustic systems, several correlations have been developed to estimate the Nusselt number (Nu), which is a dimensionless parameter quantifying the ratio of convective to conductive heat transfer in a system. These correlations take into account factors such as flow regime, heat exchanger geometry, and operating conditions. Notable examples of these correlations include the TASFE (Mozurkewich, 2001), RMS-Re (Swift, 1999), and BLC (Swift, 1992) models.

Experiments by Žukauskas (1972) led to an empirical expression (Eq. 1) that relates the Nusselt, Reynolds, and Prandtl numbers. The author suggests its applicability for various conditions, including internal airflow in a circular duct cross-flow. In the case of internal flow, the D/H ratio must be respected, where D represents the diameter of the inner duct, and H is the length of the external walls adjacent to the duct.

$$NuPr^{-0.37} = \begin{cases} 0.75\,Re^{0.4}, & 1 < Re < 40 \\ 0.51\,Re^{0.5}, & 40 < Re < 1000 \\ 0.26\,Re^{0.6}, & 1000 < Re < 20\,000 \end{cases} \tag{1}$$

The expression derived by Žukauskas (1972) was obtained for free-flow conditions under common circumstances. However, based on this equation, Mozurkewich (2001) proposed an alternative relationship that considers the effect resulting from the oscillatory movement of air in the waveguide. The estimation of heat transfer from transverse tubes using the TASFE (Time-Average Steady-Flow Equivalent) approach was derived from the corresponding correlation established for steady flow conditions. By assuming a range for the Reynolds number from 0 to $Re_1 \sin(2\pi ft)$, and performing a temporal average over half a period, Mozurkewich (2001) obtained the following expression:

$$\log_{10}\left(Nu\,Pr^{-0.37}\right) = -0.2065 + 0.3369x + 0.03322x^2, \tag{2}$$

where $x = \log_{10}(Re_1)$. According to the studies conducted by Mozurkewich (2001) and Piccolo and Pistone (2006), the expression in Eq. (2) is effective only for low Reynolds numbers. Specifically, the authors stated that it performs well within an approximate range $Re_1 < 1000$.

Regarding flow regime, Merkli and Thomann (1975) identified a critical Reynolds number around 400 for oscillatory flows, marking the onset of turbulence. However, Saat and Jaworski (2017b) observed a potential critical range of $70 < Re < 100$, suggesting possible turbulent behavior in heat exchangers. Based on Merkli and Thomann (1975), the Reynolds number is given by Eq. (3):

$$Re = \frac{2u}{\sqrt{\nu\omega}}, \tag{3}$$

where u is the amplitude of the acoustic velocity, ν is the kinematic viscosity of the gas, and ω is the angular frequency, defined as $\omega = 2\pi f$ (Shi *et al.*, 2010).

As discussed earlier, this work aims to validate a computational model of a simple heat exchanger, with water as the refrigerant flowing through a circular cross-sectional duct. This model will subsequently be adapted for more complex applications, using ferrofluid as the refrigerant flowing through an elliptical cross-sectional duct under the influence of a magnetic field. The objective is to maximize heat transfer by increasing the surface area of the duct in contact with the air in an acoustic regime and inducing greater movement of the refrigerant particles through electromagnetic force.

Elliptical cross-sectional ducts in heat exchangers, as discussed by Lin *et al.* (2023) and Yogesh *et al.* (2018), aim to increase the contact area on the duct's surface separating two fluids, while retaining a constant cross-sectional area similar to a duct with a circular section. The objective is ensuring consistent volumetric flow regardless of duct shape.

The study conducted by Lin *et al.* (2023) involved an analysis of heat transfer in an inclined tube-bank heat exchanger with an elliptical cross-section. The study considered the thermoacoustic effects in the region outside the tubes. In the study conducted by Yogesh *et al.* (2018), which did not consider thermoacoustic effects, the authors observed an improvement in heat transfer compared to circular tubes. Specifically, a significant improvement was observed when the tubes were inclined at an angle of 20 degrees. However, a pressure drop was also observed.

Regarding thermomagnetism, the interest in studying this phenomenon in heat transfer is related to the idea of maximizing the advection of the refrigerant fluid in the heat exchanger. By using ferrofluid under the influence of a magnetic field, particle oscillations occur, resulting in increased fluid flow movement. The expectation with this phenomenon is to achieve more efficient heat transfer. Studies such as those conducted by Ghosh *et al.* (2022) and Lajvardi *et al.* (2010) discuss this phenomenon through analytical and experimental approaches.

The results obtained by Ghosh *et al.* (2022) showed that with increased magnetic field strength and nanoparticle concentration, the Nusselt number decreases, despite enhanced thermal transport. This is due to intensified magnetic fields increasing viscosity and thermal conductivity. The increased viscosity negatively impacts fluid motion, while the enhanced thermal conductivity facilitates heat transfer by creating a conductive pathway. Overall, intensified conduction offsets the Nusselt number reduction.

As for the study conducted by Lajvardi *et al.* (2010), it was observed that in laminar flow, magnetic nanoparticles in water do not enhance heat transfer without a magnetic field. However, introducing a magnetic field and increasing nanoparticle volume enhances the heat transfer coefficient. Further enhancements are achieved by increasing the magnetic field strength and ferrofluid concentration. These improvements can be attributed to the magnetic field's effect on the ferrofluid's thermophysical properties.

In the end, it will be interesting to investigate how the heat transfer rate will behave when all the mentioned factors are coupled in the same system, combining thermoacoustics and thermomagnetism with an elliptical cross-section duct in the heat exchanger. The coupling of these phenomena promises to provide a complex interaction between thermoacoustic oscillations and the motion induced by the magnetic properties of the ferrofluid. This interaction has the potential to lead to an additional improvement in the heat exchanger efficiency, as the heat transfer of the refrigerant fluid is maximized by both the thermoacoustic action and the magnetic movement of the ferrofluid particles.

This work follows a previous study conducted by Bannwart *et al.* (2013), where transfer matrices were used for measurements in the thermoacoustic core. Previously, the low-temperature heat exchangers consisted of two 1/8" diameter copper tubes inside an aluminum tube. Heat exchanges from these configurations were treated implicitly together in the transfer matrices, unlike the current investigation. In this study, heat exchanges are considered individually, accounting for each system component's unique characteristics. This approach allows a more precise analysis of the heat exchanger's acoustic and thermal performance.

Ferro and Bannwart (2020) continued the study conducted by Bannwart *et al.* (2013) by performing a simulation using the DeltaEC software, which operates under Rott's approach. The main objective was to uncover variables that had previously been hidden within the measured transfer matrices of the thermoacoustic core. The ultimate goal was to enhance the efficiency and capacity of low-grade energy regeneration. The work carried out by the authors contributed to the development of a simulation in DeltaEC that was conducted simultaneously with this study.

3. METHODOLOGY

In this study, we analyze a cross-flow heat exchanger in a thermoacoustic engine using computational modeling and experimental investigation. Both methods evaluate the temperature variations within the exchanger. Numerically, values for temperature variations between the inlet and outlet for the gas under acoustic conditions and for the refrigerant fluid are determined. For the experimental approach, the collected values correspond to the temperatures at the inlet and outlet of both fluids.

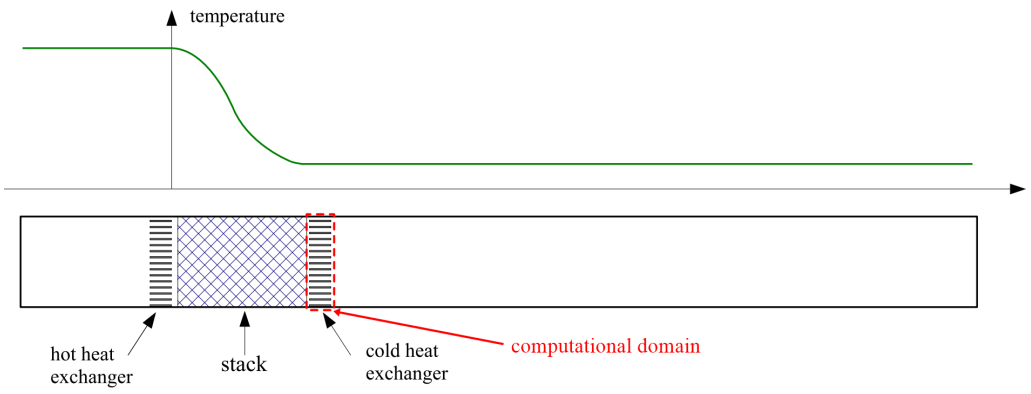

Figure 1. Schematic representation of a standing-wave thermoacoustic engine. Adapted from Bannwart (2014).

The geometry of the model under analysis consists of a heat exchanger inserted in a waveguide (Fig. 1). The waveguide has an internal circular section with a diameter of 38 mm and a length of 900 mm. The walls of the waveguide are considered thermally insulated to prevent heat exchange with the external environment, making the wall thickness irrelevant for the analysis. Inside it, positioned perpendicular to the waveguide, there is a copper tube through which water flows as a refrigerant fluid in cross-flow to the air. The copper tube has an external circular section with a diameter of 6.35 mm and a thickness of 0.79 mm, resulting in an internal diameter of 4.77 mm.

The values for the properties that govern the flows of the thermoacoustic engine used in this study, as well as their boundary conditions, was defined based on a model developed through DeltaEC software. Through this model conceived in DeltaEC, it was established the necessary parameters for simulating the heat exchanger via CFD, including pressure, frequency, and other operational properties.

3.1 Experimental setup

Experiments were conducted considering air, in free-flow conditions, exchanging heat in crossflow with water flowing through a copper tube. Conducting these experiments is essential to validate the developed computational model, especially when it is intended to be used in future studies to evaluate applications under different configurations. A well-executed experiment allows for the acquisition of accurate temperature data of the fluids in the tubes, enabling the calculation of the heat exchanged based on observed temperature variations. In this way, the experiments support the computational model providing reliability to its implementation.

The experimental setup was constructed with a PVC pipe with an external diameter of 48 mm and a thickness of 5 mm, resulting in an internal diameter of 38 mm through which air flows at a speed of 13.5 m/s and a temperature of 60ºC at the inlet. The PVC pipe is 90 cm long. At the tube's inlet, a heat blower initiates the air flow, while at the exit end, the tube is open to the atmosphere.

Inside the PVC pipe, a copper tube is positioned perpendicular to 5 cm from its inlet. Within the copper tube, water flows at room temperature (28ºC) and with a volumetric flow rate of 1.2 L/min. The copper tube was considered for two different internal sections: circular and elliptical. For the circular section tube, a 1/4" tube with a thickness of 0.79 mm was used, having an internal diameter of 4.77 mm. For the tube with an elliptical section, a 1/2" circular tube was flattened into an elliptical shape until it achieved an internal section area equivalent to the 1/4" circular tube. The dimensions of the elliptical tube were previously calculated, keeping its original perimeter and considering the internal area of the 1/4" tube.

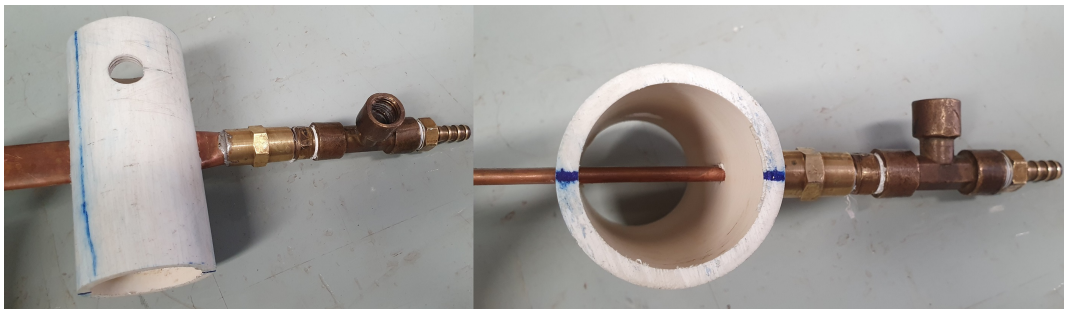

Figure 2. Elliptical copper tube heat exchanger, perpendicular and in cross-flow to air in the PVC pipe.

Temperature data collection at the inlets and outlets of the fluids was carried out using PT100 RTD temperature sensors. In the PVC pipe, one PT100 was positioned 3 cm after the air inlet and another 5 cm before the air outlet. In the copper tubes, the PT100 temperature sensors were installed 4 cm before the water inlet and 4 cm after the water outlet.

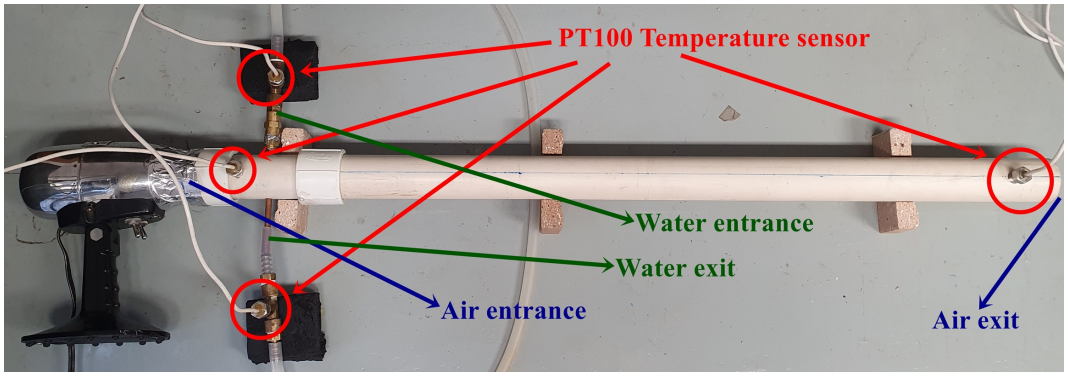

Figure 3. Heat exchanger setup including a PVC pipe with a copper tube inside and PT100 for temperature measurement.

The development length of the boundary layer in the flow was partially considered, focusing especially on its initial phase, which is the most relevant one. To mitigate potential vortex wake effects caused by the copper tube, the instrumentation at the end of the waveguide was positioned perpendicular to the copper tube, although 80 cm downstream, as shown in Fig. 3.

The data were acquired and processed using an RTD Data Acquisition Module. Each acquisition cycle extended for approximately 30 minutes, a time span both sufficient and necessary to achieve a steady-state condition, leading to minimal deviations in the temperature measurements throughout the operational sequence.

3.2 Computational model

The computational modeling of the heat exchanger was performed using the ANSYS® Fluent software, student 2022R2 version. For the computational calculation, an Intel® Core™ i5-1135G7 CPU with 4 cores, 16 GB RAM, and integrated Intel® Iris® Xe Graphics was utilized. The model development included the geometry construction, mesh generation, solution processing, and post-processing analysis. The CFD model was developed to analyze the temperature variation and heat transfer between the two fluids occurring within the heat exchanger.

The computational model was aligned with experimental data by comparing values from both methods, considering free-flowing air from prior analysis and using consistent properties, dimensions, and conditions like fluid velocity and temperature. Computational results for free-flowing air are in the Results and Discussions section in Tables 1 and 2, comparing them with experimental findings. From this, the model is evolved to consider oscillatory air regimes, capturing the effects of the thermoacoustic phenomenon.

Now considering air in the oscillatory regime, the computational domain was defined as a geometry consisting of a waveguide through which the oscillatory motion of air from the thermoacoustic phenomenon occurs, and internally within the waveguide, a tube through which water flows to reject heat. The values for the geometry dimensions were applied as described before. Figure 4 illustrates the geometry of the computational domain developed for the heat exchanger.

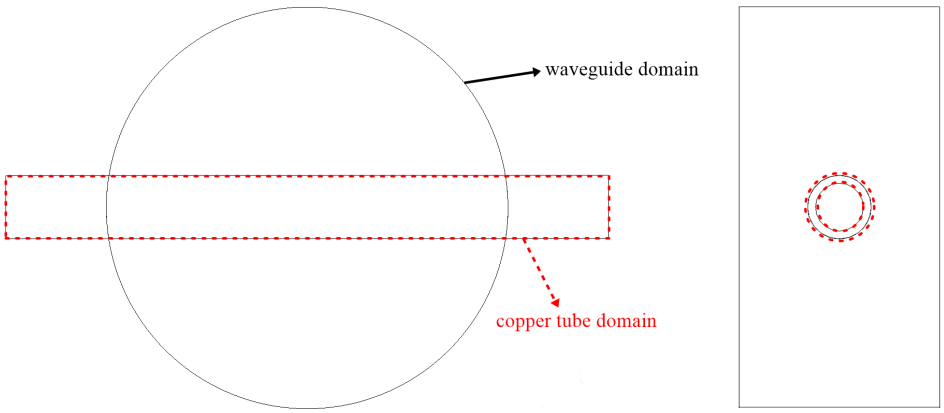

Figure 4. Geometry for the computational domain of the thermoacoustic engine heat exchanger.

An unstructured mesh was chosen because of the geometry's complexity. Mesh quality and resolution were optimized for precise representation of flow and heat transfer in the heat exchanger, especially near-wall regions where refinement occurs. The domain was discretized into approximately 270,000 elements for the analyses. Mesh independence analysis wasn't conducted due to Ansys student version limitations on element count and computational cores.

In the solution processing settings, a unsteady laminar model was chosen to solve the flow field. It is worth noting that in this study, we are not interested in analyzing the fluid dynamics involved in the process, but rather in developing a simple model that yields consistent results with those obtained experimentally regarding the heat transfer in the heat exchanger. Additionally, the calculated Reynolds number value was $Re < 1$, which is well below the critical value suggested by Saat and Jaworski (2017b), and can be considered as laminar flow.

Addressing the flow dynamics in an oscillatory regime induced by thermoacoustic phenomena presents significant challenges due to the intricate nature of the problem and the relatively unexplored research field. It is essential to establish suitable boundary conditions for the waveguide in the thermoacoustic engine to fulfill the requirement for oscillatory flow. Computational modeling, employing the Computational Fluid Dynamics (CFD) technique for a laminar fluid flow model, utilizes the governing equations of Continuity, Momentum, and Energy (White, 2011).

To properly represent the oscillatory motion of particles in a thermoacoustic regime, it is necessary to establish boundary conditions in the computational domain that accurately describe this behavior. In this regard, it is possible to consider periodic functions for the specific mass, pressure and fluid velocity, and apply them to the continuity and momentum equations, resulting in expressions for oscillating pressure and velocity. This allows for a coherent representation of the oscillatory motion of particles in the thermoacoustic context. A more detailed deduction was

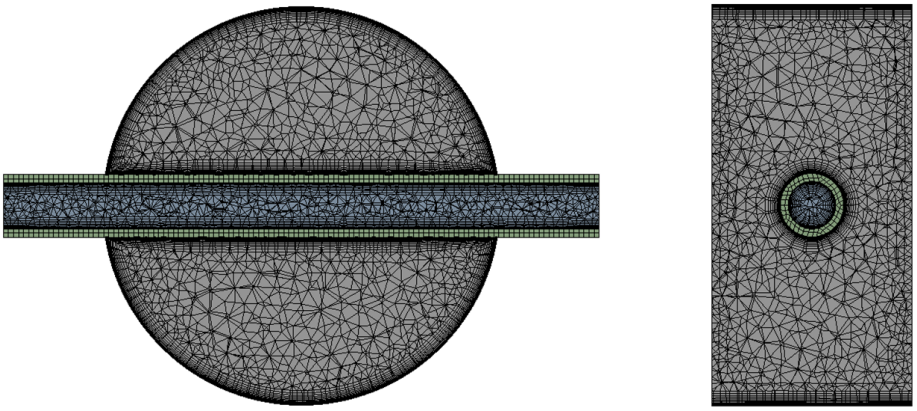

Figure 5. Mesh generated for the computational domain for the circular copper tube case.

developed by Rahpeima and Ebrahimi (2019), or similarly by Allafi and Saat (2022), which yielded the following relationships:

$$u_1 = \frac{P_a}{\rho c} \sin(k_a x_1) \cos(2\pi f t + \theta), \tag{4}$$

$$P_2 = P_a \cos(k_a x_2) \cos(2\pi f t), \tag{5}$$

where u_1 and P_2 represent the oscillatory air pressure and velocity, respectively. P_a is the acoustic pressure at the location of the pressure antinode, k_a is the wave number, f is the frequency, c is the speed of sound, and θ is the phase angle between pressure and velocity. The terms x_1 and x_2 represent the locations of the inlet and outlet applied in the boundary conditions, while t refers to the temporal variable (Allafi and Saat, 2022).

It should be noted that the waveguide contains an area filled with air that is affected by thermoacoustic phenomena. Specifically within this designated control volume, the net velocity balances out to zero over a complete cycle due to the standing wave condition. Therefore, Eqs. (4) and (5) were utilized, with Eq. (4) describing the oscillatory air velocity u_1 at the inlet, while Eq. (5) represents the oscillatory pressure P_2 at the outlet of the control volume corresponding to the waveguide.

For u_1 and P_2, the values of the variables and properties in the equations were established as follows: $P_a = 5$ Pa, $k_a = 1.998$ m^{-1}, $x_1 = 0.195$ m, $x_2 = 0.215$ m, $f = 110$ Hz, $c = 346$ m/s, $\theta = 85$ deg. These values were taken as reference from a parallel study being conducted in the DeltaEC software. The air temperature at the inlet of the heat exchanger was defined as 60ºC, same as in the experiment with air in the free-flow condition.

Another region that requires the insertion of boundary conditions is the one corresponding to the tube through which the refrigerant fluid flows in the heat exchanger. In this case, water is used as the refrigerant fluid in free-flow conditions, without oscillatory effects. Thus, a volumetric flow rate condition of 1.2 L/min was set at the inlet, and a gauge pressure of 0 Pa at the outlet of the control volume. The fluid temperature at the inlet was defined as the ambient temperature, considered to be 28ºC in this case.

For the pressure-velocity coupling, the pressure-based solver Pressure-Implicit with Splitting Operators (PISO) algorithm was adopted, as it was used by Allafi and Saat (2022), Saat *et al.* (2019), Ilori *et al.* (2018), Yu *et al.* (2010), and others in similar analyses. A second-order upwind scheme was also employed to solve the transient formulation and the spatial discretization of pressure and momentum.

Since the flow condition was defined as unsteady, it is necessary to determine the time step size in the numerical calculation. In studies conducted by Allafi *et al.* (2021), Mustaffa *et al.* (2017), and Saat and Jaworski (2017a), a time step size corresponding to the ratio $\Delta t = 1/1200f$ was employed, which represents the calculation of 1200 time steps to achieve one complete period. This ratio was considered suitable for convergence in previous studies and therefore will be used in this study for the adopted frequency.

The number of time steps was defined to be equivalent to 15 complete periods of air oscillation, aiming to obtain a quasi-steady solution. This approach is particularly relevant for problems where achieving a truly steady-state solution is challenging due to the inherent transient or oscillatory nature. In such cases, fluid flow problems tend to approach a quasi-steady state, where changes between consecutive periods are minimal, accurately capturing the dominant periodic behavior of the fluid flow. The decision to employ a quasi-steady approach ensures a balance between accuracy and computational efficiency.

For the purpose of comparison with the case of a circular cross-section copper tube, a computational model with similar geometry was developed. In this alternative model, the copper tube has an elliptical cross-section, but with an internal area equivalent to that of the circular cross-section tube, which is approximately 17.9 mm^2. The fundamental

purpose of this analysis is to investigate whether there is an increase in heat transfer rate to the air, considering that the external surface area of the copper tube in contact with the air is larger when the tube is flattened in an elliptical shape.

4. RESULTS AND DISCUSSION

The experimental and computational approaches, considering free-flowing air, exhibited minor temperature variations between the fluid's inlet and outlet, both for the copper tube with a circular internal section and for the elliptical one. Moreover, there was a close match between the actual and the simulated values. The experimental and computational results, with free-flowing air, are listed in Table 1 for the circular case and in Table 2 for the elliptical case.

Table 1. Experimental and computational temperature values obtained for the circular copper tube case.

Temperature values obtained	$T_{in,water}$	$T_{out,water}$	ΔT_{water}	$T_{in,air}$	$T_{out,air}$	ΔT_{air}
Experiment, ^{o}C	28.00	28.14	0.14	60.00	59.66	-0.34
CFD, ^{o}C	28.00	28.13	0.13	60.00	59.83	-0.17

Table 2. Experimental and computational temperature values obtained for the elliptical copper tube case.

Temperature values obtained	$T_{in,water}$	$T_{out,water}$	ΔT_{water}	$T_{in,air}$	$T_{out,air}$	ΔT_{air}
Experiment, ^{o}C	28.00	28.35	0.35	60.00	59.53	-0.47
CFD, ^{o}C	28.00	28.17	0.17	60.00	59.80	-0.20

The difference in temperature variations between the experiment and the simulation can be attributed to heat transfer losses present in the experiment, but not accounted for in the simulation. These losses occur, for instance, in the segment of the copper tube exposed to the air and along the waveguide. Even though the waveguide is made of a material with low thermal conductivity, it still dissipates significant heat through natural convection when in a steady-state regime.

When examining the case with air in an oscillatory regime, the computational results indicated that the oscillatory behavior was effectively replicated using the equations and methods proposed by Rahpeima and Ebrahimi (2019) and Allafi and Saat (2022). Fig. 6 displays the velocity field vectors at maximum amplitude in both negative and positive directions of the axis for (a) the circular copper tube and (b) the elliptical copper tube, where the oscillatory flow is evident. This suggests that the computational model adeptly simulates the system's behavior, capturing the inherent oscillations of the heat transfer process in the heat exchanger.

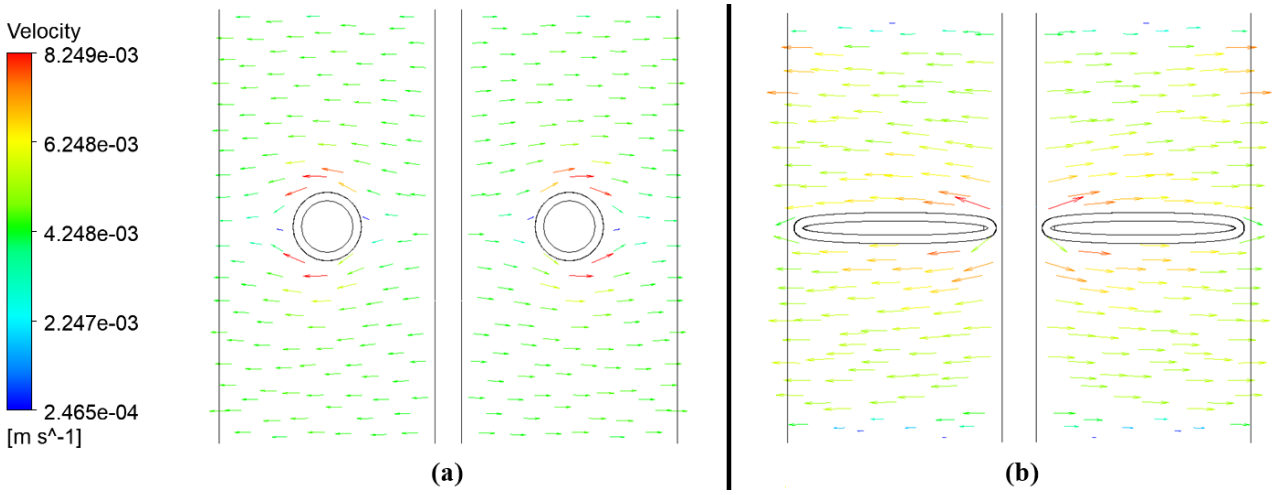

Figure 6. Velocity field representing the amplitude of the oscillatory flow.

It is worth noting that there is no net mass flux in the air flow since, under the condition of standing wave, the air particles oscillate around a fixed midpoint.

Temperature contours were obtained and can be found in Fig. 7. These contours were extracted from the cross-sections of the **(a)** waveguide and **(b)** copper tube, at the center of their respective longitudinal axes. It can be observed in the figure that heat transfer occurs mainly through conduction, with little noticeable advection due to the low velocity amplitudes in the flows and consequently low Reynolds numbers. Natural convection does not occur as gravity acceleration was not considered in this initial calculation.

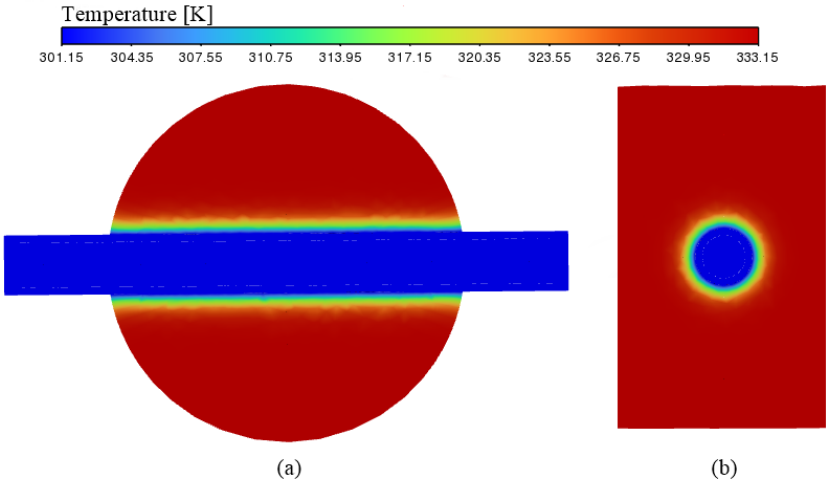

Figure 7. Temperature contours in the cross-sections at the center of (a) waveguide and (b) copper tube.

Temperature contours for the case of the tube with an elliptical cross-section were also obtained and are presented in Fig. 8. The visualization of the figure reveals, once again, that thermal conduction prevails over the advection effect, due to the low velocity of the two fluids. Considering that our objective is to specifically investigate the influence of variations in geometry and flow characteristics on advection properties, it becomes necessary to adjust the model in order to make the advection phenomenon more prominent and perceptible.

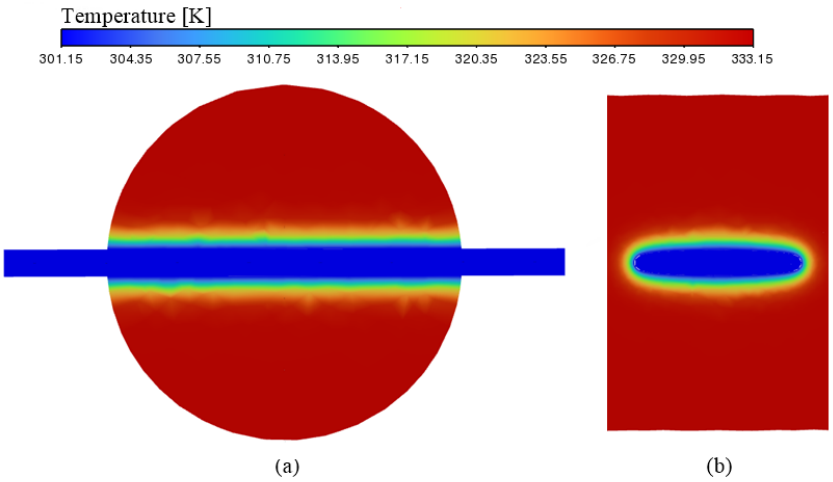

Figure 8. Temperature contours for the case of the tube with an elliptical cross-section.

The temperature values of the air at the boundaries of the computational domain, as well as at the water inlet and outlet, are detailed in Table 3.

Table 3. Computational temperature values obtained for the circular and the elliptical copper tube cases.

Temperature values obtained	$T_{in,water}$	$T_{out,water}$	ΔT_{water}	$T_{in,air}$	$T_{out,air}$	ΔT_{air}
Circular copper tube, ^{o}C	28.00	28.15	0.15	60.00	59.71	-0.29
Elliptical copper tube, ^{o}C	28.00	28.21	0.21	60.00	59.58	-0.42

In the absence of an experiment with a thermoacoustic engine fully operating with air particles in resonance, Eq. (2) was used to calculate the Nusselt number, allowing for comparison with the value obtained through simulation for the copper tube with a circular section. There was no agreement in the results from both approaches. From the CFD analysis, the Nusselt number was 4.24, while the empirical expression yielded a value of 0.69. Two hypotheses arise: the mesh elements in the thermal exchange region were not adequately discretized, or a greater number of periods in the transient calculation might be needed to better represent the quasi-steady regime. These hypotheses will be further investigated in the future.

Even still, the results obtained so far provide a promising foundation for future investigations and experimental validations of the model.

5. CONCLUSIONS

The simulations with air in the thermoacoustic condition demonstrated the model's effectiveness in capturing the oscillatory characteristics of heat transfer in the heat exchanger. Figure 6 depicts the velocity distributions, showcasing the model's capability to accurately simulate the system's behavior. Additionally, the temperature contours in Fig. 7 and Fig. 8 indicates that heat transfer occurs predominantly through conduction, with minimal notable advection due to low velocity amplitudes.

It's important to note that in all the analyzed scenarios, the comparison between the tubes with elliptical and circular sections revealed greater thermal exchange effectiveness for the elliptical tube, producing more significant temperature variations between the inlets and outlets of the control volumes when compared to the cases with the circular tube.

Furthermore, at the present investigation it was not feasible to conduct an experiment with the thermoacoustic engine to replicate the phenomenon of air in an oscillatory regime and allow a direct comparison with the computational model developed in this study. However, the initial validation considering the air in free flow, combined with the consistency of the simulation results with oscillating air, makes the findings satisfactory at this initial stage.

Supplementing this study with experimental data from an analysis with a thermoacoustic engine operating at full capacity with oscillating air will enhance the robustness of the evaluation of heat transfer in the heat exchanger. It will establish greater reliability in the computational results and ensure compatibility between the approaches. This, in turn, will lead to a more comprehensive understanding of the studied phenomenon and result in more solid conclusions for future researches.

The results achieved in this study will significantly contribute to advancements in research and the implementation of computational calculations involving geometries and refrigerant fluids under more complex conditions, such as in the application of ferrofluid influenced by a magnetic field aiming for coupling with air's acoustic particles. Thus, the findings obtained lay a solid foundation for future investigations in the field.

6. ACKNOWLEDGEMENTS

This study was financed in part by the Coordenação de Aperfeiçoamento de Pessoal de Nível Superior - Brasil (CAPES) - Finance Code 001, so we would like to thank them, as well as the School of Mechanical Engineering for providing the support and infrastructure for the development of this research.

7. REFERENCES

Alamir, M.A., 2021. "Thermoacoustic energy conversion devices: Novel insights". *Journal of Advanced Research in Fluid Mechanics and Thermal Sciences*, Vol. 77, pp. 130–144.

Allafi, W.A. and Saat, F.A.Z.M., 2022. "Entrance and exit effects on oscillatory flow within parallel-plates in standing-wave thermoacoustic system with two different operating frequencies". *Journal of King Saud University – Engineering Sciences*, Vol. 77, pp. 350–360.

Allafi, W.A., Saat, F.A.Z.M. and Mao, X., 2021. "Fluid dynamics of oscillatory flow across parallel-plates in standing-wave thermoacoustic system with two different operation frequencies". *Engineering Science and Technology, an International Journal*, Vol. 24, pp. 41–49.

Bannwart, F.C., 2014. *Methods for the transfer matrix evaluation of thermoacoustic cores with application to the design of thermoacoustic engines*. Ph.D. thesis, Thesis (Doctorate). Faculdade de Engenharia Mecânica, Universidade Estadual de Campinas, Campinas, SP, Brasil.

Bannwart, F.C., Penelet, G., Lotton, P. and Dalmont, J.P., 2013. "Measurements of the impedance matrix of a thermoacoustic core: Applications to the design of thermoacoustic engines". *Journal of the Acoustical Society of America*, Vol. 133, pp. 2650–2660.

Chen, G., Tang, L. and Mace, B.R., 2018. "Theoretical and experimental investigation of the dynamic behaviour of a standing-wave thermoacoustic engine with various boundary conditions". *International Journal of Heat and Mass Transfer*, Vol. 123, pp. 367–381.

Ferro, B. and Bannwart, F.C., 2020. "Modeling a thermoacoustic engine under rott's approach from experimental transfer matrices of a thermoacoustic core". In *18th Brazilian Congress of Thermal Sciences and Engineering*. Associação Brasileira de Engenharia e Ciências Mecânicas (ABCM), Online Event.

Ghosh, D., Meena, P.R. and Das, P.K., 2022. "A fully analytical solution of convection in ferrofluids during couette-poiseuille flow subjected to an orthogonal magnetic field". *International Communications in Heat and Mass Transfer*, Vol. 130.

Ilori, O.M., Jaworski, A.J. and Mao, X., 2018. "Experimental and numerical investigations of thermal characteristics of heat exchangers in oscillatory flow". *Applied Thermal Engineering*, Vol. 144, pp. 910–925.

Jaworski, A.J. and Mao, X., 2013. "Development of thermoacoustic devices for power generation and refrigeration". *Proceedings of the Institution of Mechanical Engineers, Part A: Journal of Power and Energy*, Vol. 227, pp. 762–782.

Jaworski, A.J. and Piccolo, A., 2012. "Heat transfer processes in parallel-plate heat exchangers of thermoacoustic devices - numerical and experimental approaches". *Applied Thermal Engineering*, Vol. 42, pp. 145–153.

Lajvardi, M., Moghimi-Rad, J., Hadi, I., Gavili, A., Isfahani, T.D., Zabihi, F. and Sabbaghzadeh, J., 2010. "Experimental investigation for enhanced ferrofluid heat transfer under magnetic field effect". *Journal of Magnetism and Magnetic Materials*, Vol. 322, pp. 3508–3513.

Lin, C.A., Saat, F.A.Z.M. and Anuar, F.S., 2023. "Heat transfer for the oscillatory flow of thermoacoustics across an in-line tube-banks heat-exchanger". *Heat Transfer Engineering*, Vol. 44, pp. 865–883.

Merkli, P. and Thomann, H., 1975. "Transition to turbulence in oscillating pipe flow". *Journal of Fluid Mechanics*, Vol. 68, pp. 567–575.

Mozurkewich, G., 2001. "Heat transfer from transverse tubes adjacent to a thermoacoustic stack". *J Acoust Soc Am*, Vol. 110, p. 841–847.

Mumith, J.A., Makatsoris, C. and Karayiannis, T.G., 2014. "Design of a thermoacoustic heat engine for low temperature waste heat recovery in food manufacturing: A thermoacoustic device for heat recovery". *Applied Thermal Engineering*, Vol. 65, pp. 588–596.

Mustaffa, S.H.A., Saat, F.A.Z.M. and Tokit, E.M., 2017. "Numerical investigation of turbulence in oscillatory flow found in thermoacoustics". In *Proceedings of Mechanical Engineering Research Day 2017*. Centre for Advanced Research on Energy, Melaka, Malaysia.

Piccolo, A. and Pistone, G., 2006. "Estimation of heat transfer coefficients in oscillating flows: The thermoacoustic case". *International Journal of Heat and Mass Transfer*, Vol. 49, pp. 1631–1642.

Piccolo, A., Sapienza, A. and Guglielmino, C., 2019. "Convection heat transfer coefficients in thermoacoustic heat exchangers: An experimental investigation". *Energies*, Vol. 12, pp. 1–10.

Rahpeima, R. and Ebrahimi, R., 2019. "Numerical investigation of the effect of stack geometrical parameters and thermo-physical properties on performance of a standing wave thermoacoustic refrigerator". *Applied Thermal Engineering*, Vol. 149, pp. 1203–1214.

Saat, F.A.Z.M. and Jaworski, A.J., 2017a. "The effect of temperature field on low amplitude oscillatory flow within a parallel-plate heat exchanger in a standing wave thermoacoustic system". *Applied Sciences*, Vol. 7 (417), pp. 1–29.

Saat, F.A.Z.M. and Jaworski, A.J., 2017b. "Numerical predictions of early stage turbulence in oscillatory flow across parallel-plate heat exchangers of a thermoacoustic system". *Applied Sciences*, Vol. 7 (673), pp. 1–22.

Saat, F.A.Z.M., Mustaffa, S.H.A. and Anuar, F.S., 2019. "Numerical and experimental investigations of the oscillatory flow inside standing wave thermoacoustic system at two different flow frequencies". *CFD Letters*, Vol. 11, pp. 1–15.

Shi, L., Yu, Z. and Jaworski, A.J., 2010. "Application of laser-based instrumentation for measurement of time-resolved temperature and velocity fields in the thermoacoustic system". *International Journal of Thermal Sciences*, Vol. 49, pp. 1688–1701.

Sun, D.M., Wang, K., Zhang, X.J., Guo, Y.N., Xu, Y. and Qiu, L.M., 2013. "A traveling-wave thermoacoustic electric generator with a variable electric R-C load". *Applied Energy*, Vol. 106, pp. 377–382.

Swift, G.W., 1992. "Analysis and performance of a large thermoacoustic engine". *Journal of the Acoustical Society of America*, Vol. 92, pp. 1551–1563.

Swift, G.W., 1999. "Thermoacoustic engines and refrigerators: A short course". URL `https://www.osti.gov/biblio/756947`.

Wang, K., Sun, D.M., Zhang, J., Zou, J., Wu, K., Qiu, L.M. and Huang, Z.Y., 2015. "Numerical simulation on onset characteristics of traveling-wave thermoacoustic engines based on a time-domain network model". *International Journal of Thermal Sciences*, Vol. 94, pp. 61–71.

White, F., 2011. *Fluid Mechanics*. McGraw-Hill, New York, NY, US.

Yogesh, S.S., Selvaraj, A.S., Ravi, D.K. and Rajagopal, T.K.R., 2018. "Heat transfer and pressure drop characteristics of inclined elliptical fin tube heat exchanger of varying ellipticity ratio using cfd code". *International Journal of Heat and Mass Transfer*, Vol. 119, pp. 26–39.

Yu, G., Dai, W. and Luo, E., 2010. "CFD simulation of a 300 Hz thermoacoustic standing wave engine". *Cryogenics*, Vol. 50, pp. 615–622.

Žukauskas, A., 1972. "Heat transfer from tubes in crossflow". *Advances in Heat Transfer*, Vol. 8, p. 93–160.

8. RESPONSIBILITY NOTICE

The authors are solely responsible for the printed material included in this paper.